

Two photon annihilation of Kaluza-Klein dark matter

Lars Bergström,^{*} Torsten Bringmann,[†] Martin Eriksson,[‡] and Michael Gustafsson[§]

Department of Physics, Stockholm University,

AlbaNova University Center, SE - 106 91 Stockholm, Sweden

(Dated: November 5, 2018)

Abstract

We investigate the fermionic one-loop cross section for the two photon annihilation of Kaluza-Klein (KK) dark matter particles in a model of universal extra dimensions (UED). This process gives a nearly mono-energetic gamma-ray line with energy equal to the KK dark matter particle mass. We find that the cross section is large enough that if a continuum signature is detected, the energy distribution of gamma-rays should end at the particle mass with a peak that is visible for an energy resolution of the detector at the percent level. This would give an unmistakable signature of a dark matter origin of the gamma-rays, and a unique determination of the dark matter particle mass, which in the case studied should be around 800 GeV. Unlike the situation for supersymmetric models where the two-gamma peak may or may not be visible depending on parameters, this feature seems to be quite robust in UED models, and should be similar in other models where annihilation into fermions is not helicity suppressed. The observability of the signal still depends on largely unknown astrophysical parameters related to the structure of the dark matter halo. If the dark matter near the galactic center is adiabatically contracted by the central star cluster, or if the dark matter halo has substructure surviving tidal effects, prospects for detection look promising.

PACS numbers:

^{*}Electronic address: lbe@physto.se

[†]Electronic address: troms@physto.se

[‡]Electronic address: mate@physto.se

[§]Electronic address: michael@physto.se

I. INTRODUCTION

The mystery of the dark matter, first indicated by Zwicky some 70 years ago [1], is still with us. Thanks to remarkably accurate measurements of the microwave background [2], supernova luminosity distances [3] and the redshift distribution of baryonic structure [4], we now have, however, a good handle on the required dark matter density of the Universe.

Among the various possibilities for the dark matter constituents, weakly interacting massive particles (WIMPs) are particularly attractive, as gauge couplings and masses in the electroweak symmetry breaking range (50 - 1000 GeV, say) give a thermal relic abundance of particles that naturally comes within the observed range. Supersymmetry or Kaluza-Klein (KK) particles in models with large extra dimensions are examples which span some of the range of the phenomenology to expect [5].

Dark matter particles can in principle be detected in three different ways: In accelerators, if the energy is high enough to produce them. Through direct detection in ultra-sensitive detectors, where particles from the local neighborhood of the halo deposit enough energy to be detected. Finally, indirectly through the contribution to the cosmic ray flux (positrons, antiprotons, neutrinos and photons of all energies up to the particle mass) caused by annihilations in the halo (or in celestial bodies for neutrinos). Here we will focus on indirect detection through high energy gamma-rays, a signal that has recently become much more interesting because of new large-area air Cherenkov telescopes (ACTs) [6, 7] and the launch of the Integral satellite [8]. In a couple of years, a new satellite, GLAST [9], will take the field of high energy gamma-ray astrophysics to yet another level of accuracy and precision.

There are many reported indications of cosmic ray signals which could in principle at least partly be due to the annihilation products of dark matter particles. Examples are possible excesses in microwave radiation [10], in positrons [11, 12] and gamma-rays from the galactic center (GC) in the MeV range [13, 14], GeV range [15, 16, 17] and TeV range [18, 19]. Indeed, there have even been suggestions that the combined data on positrons, gamma-rays and antiprotons could be better explained by adding a neutralino annihilation contribution [20].

The problem with these indications is that they lack distinctive features, which will make the alternative hypothesis that there are unknown background contributions difficult to reject. A spectacular signature would on the other hand be the mono-energetic gamma-

rays expected from WIMP annihilation into $\gamma\gamma$ [21] or $Z\gamma$ [22]. The phenomenology of this process has been worked out in quite some detail for the supersymmetric case [17, 23]. Here we present the first analytical and numerical calculations of the dominant fermion loop contributions to the process $B^{(1)}B^{(1)} \rightarrow \gamma\gamma$ for KK dark matter. This dark matter particle has recently been shown to contain a useful experimental signature in the form of a gamma-ray spectrum that remains remarkably flat up to the KK mass, and then steeply drops at that energy [24]. Here, we investigate whether there could also be a sharp peak at $E_\gamma = M_{B^{(1)}}$ due to the two-gamma process. Needless to say, there is no known astrophysical background which would cause a similar structure, so the question is only if the particle physics annihilation cross section and the dark matter halo density are large enough to make the signal visible.

The paper is organized as follows. We begin by introducing the model that gives rise to the KK dark matter candidate $B^{(1)}$. In Sections III and IV we then discuss the basic properties of the cross section and give the analytical result for the fermionic contribution. We also comment on a full numerical evaluation of the process $B^{(1)}B^{(1)} \rightarrow \gamma\gamma$ and argue that the fermionic part gives the main contribution. In Section V we insert the analytical results into a model of the Milky Way halo that represents the current knowledge based on N-body simulations and baryonic contraction near the GC. We also make some speculations on the existence of dark matter substructure (“clumps”) and finally, Section VI, contains our summary and conclusions.

II. UNIVERSAL EXTRA DIMENSIONS

The lightest KK particle (LKP) is the first viable particle dark matter candidate to arise from extra dimensional extensions of the standard model (SM) of particle physics. It appears in models of universal extra dimensions (UED) [25, 26, 27] (for the first proposal of TeV sized extra dimensions, see [28]), where all SM fields propagate in the higher dimensional bulk, and is stable due to conserved KK parity, a remnant of KK mode number conservation. This is analogous to supersymmetric dark matter models, where conserved R-parity ensures the stability of, e.g., the neutralino. Contrary to the supersymmetric case however, the unknown parameter space is quite small and will be scanned throughout by next generation’s accelerator experiments.

We will consider the simplest, five dimensional model with one UED compactified on an S^1/Z_2 orbifold of radius R . All SM fields are then accompanied by a tower of increasingly massive KK states and at tree-level, the n th KK mode mass is given by

$$m^{(n)} = \sqrt{(n/R)^2 + m_{\text{EW}}^2}, \quad (1)$$

where m_{EW} is the corresponding zero mode mass. However, the identification of the LKP is nontrivial because radiative corrections to the mass spectrum of the first KK level are typically larger than the corresponding electroweak mass shifts. A one-loop calculation [26] shows that the LKP is given by the first KK excitation of the photon, which is well approximated by the first KK mode of the hypercharge gauge boson $B^{(1)}$ since the electroweak mixing angle for KK modes is effectively driven to zero. The $B^{(1)}$ relic density was determined in [27]. Depending on the exact form of the mass spectrum and the resulting coannihilation channels, the limit from the Wilkinson Microwave Anisotropy Probe (WMAP) [2] of $\Omega_{\text{CDM}}h^2 = 0.12 \pm 0.02$ corresponds to $0.5 \text{ TeV} \lesssim m_{B^{(1)}} \lesssim 1 \text{ TeV}$. Here Ω_{CDM} is the ratio of dark matter to critical density and h is the Hubble constant in units of $100 \text{ km s}^{-1} \text{ Mpc}^{-1}$. Collider measurements of electroweak observables give a current constraint of $R^{-1} \gtrsim 0.3 \text{ TeV}$ [25, 29], whereas LHC should probe compactification radii up to 1.5 TeV [30].

Although all SM fields come with a tower of KK states, only those which are even under Z_2 have a zero mode. Fermions in five dimensions are not chiral, but chiral zero modes can still be singled out by assigning different transformation properties to the $SU(2)$ doublet and singlet, respectively. Denoting four dimensional spacetime coordinates by x^μ and the fifth coordinate by y , the fermion expansion in KK states is then given by

$$\begin{aligned} \psi_d(x^\mu, y) &= \frac{1}{\sqrt{2\pi R}} P_L \psi^{(0)}(x^\mu) + \frac{1}{\sqrt{\pi R}} \sum_{n=1}^{\infty} \left[P_L \psi_d^{(n)}(x^\mu) \cos \frac{ny}{R} + P_R \psi_d^{(n)}(x^\mu) \sin \frac{ny}{R} \right], \\ \psi_s(x^\mu, y) &= \frac{1}{\sqrt{2\pi R}} P_R \psi^{(0)}(x^\mu) + \frac{1}{\sqrt{\pi R}} \sum_{n=1}^{\infty} \left[P_R \psi_s^{(n)}(x^\mu) \cos \frac{ny}{R} + P_L \psi_s^{(n)}(x^\mu) \sin \frac{ny}{R} \right], \end{aligned} \quad (2)$$

where

$$P_{L,R} = \frac{1 \mp \gamma^5}{2}. \quad (3)$$

Thus at a given KK level, the fermionic field content is doubled as compared to the SM. In the following we neglect the zero mode fermion mass, and set the radiative mass corrections

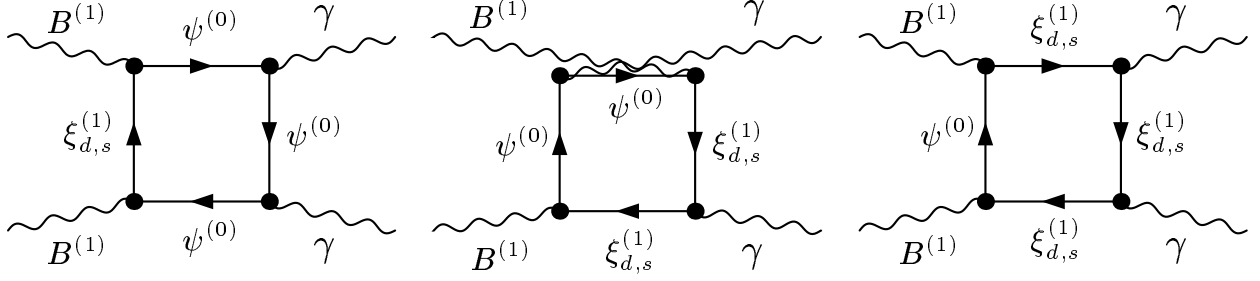


FIG. 1: Fermion box contributions to $B^{(1)}B^{(1)} \rightarrow \gamma\gamma$ including the first level of KK excitations. Not shown are the additional nine diagrams that are obtained by crossing external momenta.

to the singlet and doublet KK excitations equal. The mass eigenstates are then given by

$$\xi_d^{(n)} = \psi_d^{(n)}, \quad \xi_s^{(n)} = -\gamma^5 \psi_s^{(n)}, \quad (4)$$

which contributes a relative minus sign in the Feynman rules for $B^{(1)}$ -fermion vertices.

The number of scalar degrees of freedom is also doubled, since the fifth components of the gauge bosons transform as four dimensional scalars. These are required to be odd under Z_2 by gauge invariance. The KK excitations of Z_5 and W_5^\pm combine with those of the three Goldstone bosons of the SM to form three physical and three unphysical scalars, the latter giving masses to $Z_\mu^{(n)}$ and $W_\mu^{\pm(n)}$. The KK photon acquires a mass by eating A_5 , while the Higgs excitations remain physical.

III. THE $B^{(1)}B^{(1)} \rightarrow \gamma\gamma$ POLARIZATION TENSOR

Let us now discuss the direct annihilation of $B^{(1)}$ particles into photons. Taking all momenta as ingoing, the amplitude for this process is given by

$$\mathcal{M} = \epsilon_1^{\mu_1}(p_1)\epsilon_2^{\mu_2}(p_2)\epsilon_3^{\mu_3}(p_3)\epsilon_4^{\mu_4}(p_4)\mathcal{M}_{\mu_1\mu_2\mu_3\mu_4}(p_1, p_2, p_3, p_4), \quad (5)$$

where $p_{1,2}$ and $p_{3,4}$ denote the four-momenta of the $B^{(1)}$ s and photons with polarization vectors $\epsilon_1, \dots, \epsilon_4$, respectively.

Let us first consider those contributions to the polarization tensor that do not contain scalars. At the one-loop level, and taking into account only the first level of KK-excitations, they are given by the fermion box diagrams that are shown in Fig. 1. Photons couple to the charge of the KK fermions by the usual vector coupling, while the couplings of the $B^{(1)}$ s to

fermions contains a vector as well as an axial vector part and is given by

$$-g_Y \frac{Y_s}{2} B_\mu^{(1)} \bar{\xi}_s^{(1)} \gamma^\mu (1 + \gamma^5) \psi^{(0)} + c.c. \quad (6)$$

and

$$g_Y \frac{Y_d}{2} B_\mu^{(1)} \bar{\xi}_d^{(1)} \gamma^\mu (1 - \gamma^5) \psi^{(0)} + c.c. , \quad (7)$$

respectively. Here, $\psi^{(0)}$ is a zero level fermion and $\xi_s^{(1)}$ ($\xi_d^{(1)}$) its first singlet (doublet) KK excitation with hypercharge Y_s (Y_d) as explained above. From charge conjugation invariance it follows that there is no total axial vector contribution to the process (i.e. no remaining γ^5 in the trace). This means that the polarization tensor can be written as

$$\mathcal{M}^{\mu_1 \mu_2 \mu_3 \mu_4} = -i \alpha_{em} \alpha_Y Q^2 (Y_s^2 + Y_d^2) (\mathcal{M}_v^{\mu_1 \mu_2 \mu_3 \mu_4} + \mathcal{M}_a^{\mu_1 \mu_2 \mu_3 \mu_4}) , \quad (8)$$

where we have pulled out a common factor for later convenience, with $\alpha_{em} \equiv e^2/4\pi$, $\alpha_Y \equiv g_Y^2/4\pi$ and Q being the charge of the fermions in the loop. In the above expression, \mathcal{M}_v describes the contributions from vector couplings only, whereas \mathcal{M}_a comes from those terms that only contain $B^{(1)}$ axial vector couplings. In our case, with the couplings given by (6) and (7),

$$\mathcal{M}_v^{\mu_1 \mu_2 \mu_3 \mu_4} = \mathcal{M}_a^{\mu_1 \mu_2 \mu_3 \mu_4} . \quad (9)$$

The typical velocity of WIMPs is about $v \sim 10^{-3}$, i.e. they are highly non-relativistic. The momenta of the incoming $B^{(1)}$ s are therefore well approximated by $p \equiv p_1 = p_2 = (m_{B^{(1)}} \mathbf{0})$. Taking into account momentum conservation,

$$2p^\mu + p_3^\mu + p_4^\mu = 0, \quad (10)$$

and transversality of the polarization vectors,

$$\epsilon_1 \cdot p = \epsilon_2 \cdot p = \epsilon_3 \cdot p_3 = \epsilon_4 \cdot p_4 = 0, \quad (11)$$

the Lorentz structure of the polarization tensor can be decomposed as

$$\begin{aligned} \mathcal{M}_v^{\mu_1 \mu_2 \mu_3 \mu_4} = & \frac{A}{m_{B^{(1)}}^4} p_3^{\mu_1} p_4^{\mu_2} p^{\mu_3} p^{\mu_4} + \frac{B_1}{m_{B^{(1)}}^2} g^{\mu_1 \mu_2} p^{\mu_3} p^{\mu_4} + \frac{B_2}{m_{B^{(1)}}^2} g^{\mu_1 \mu_3} p_4^{\mu_2} p^{\mu_4} \\ & + \frac{B_3}{m_{B^{(1)}}^2} g^{\mu_1 \mu_4} p_4^{\mu_2} p^{\mu_3} + \frac{B_4}{m_{B^{(1)}}^2} g^{\mu_2 \mu_3} p_3^{\mu_1} p^{\mu_4} + \frac{B_5}{m_{B^{(1)}}^2} g^{\mu_2 \mu_4} p_3^{\mu_1} p^{\mu_3} \\ & + \frac{B_6}{m_{B^{(1)}}^2} g^{\mu_3 \mu_4} p_3^{\mu_1} p_4^{\mu_2} + C_1 g^{\mu_1 \mu_2} g^{\mu_3 \mu_4} + C_2 g^{\mu_1 \mu_3} g^{\mu_2 \mu_4} + C_3 g^{\mu_1 \mu_4} g^{\mu_2 \mu_3} , \quad (12) \end{aligned}$$

where A , B and C are dimensionless scalars that depend on the external momenta and the masses appearing in the loop.

Bose symmetry prescribes that the tensor must be invariant under the permutations $(p_1, \mu_1) \leftrightarrow (p_2, \mu_2)$ and $(p_3, \mu_3) \leftrightarrow (p_4, \mu_4)$. This translates into

$$\begin{aligned}
B_2 &= -B_4, \\
B_3 &= -B_5, \\
C_2 &= C_3, \\
A(3, 4) &= A(4, 3), \\
B_1(3, 4) &= B_1(4, 3), \\
B_2(3, 4) &= -B_3(4, 3), \\
B_6(3, 4) &= B_6(4, 3), \\
C_1(3, 4) &= C_1(4, 3), \\
C_2(3, 4) &= C_3(4, 3),
\end{aligned} \tag{13}$$

where we have introduced the notation $A(3, 4) \equiv A(p, p_3, p_4)$, $A(4, 3) \equiv A(p, p_4, p_3)$ etc.

Because of gauge invariance the polarization tensor furthermore has to be transversal to the photon momenta, i.e.

$$\epsilon_1^{\mu_1} \epsilon_2^{\mu_2} p_3^{\mu_3} \epsilon_4^{\mu_4} \mathcal{M}_{\mu_1 \mu_2 \mu_3 \mu_4} = \epsilon_1^{\mu_1} \epsilon_2^{\mu_2} \epsilon_3^{\mu_3} p_4^{\mu_4} \mathcal{M}_{\mu_1 \mu_2 \mu_3 \mu_4} = 0. \tag{14}$$

This gives

$$\begin{aligned}
A &= B_2 - B_4 - 2B_6, \\
C_1 &= -\frac{1}{2}B_1, \\
C_2 &= B_5, \\
C_3 &= -B_3.
\end{aligned} \tag{15}$$

With the help of Eqs. (13) and (15) one can express the whole tensor amplitude by means of only three form factors, which we choose to be B_1 , B_2 and B_6 . The full analytical expressions for these functions are given in the Appendix . We actually calculated *all* the form factors A , B and C independently and used Eqs. (13) and (15) merely as a consistency check of our results.

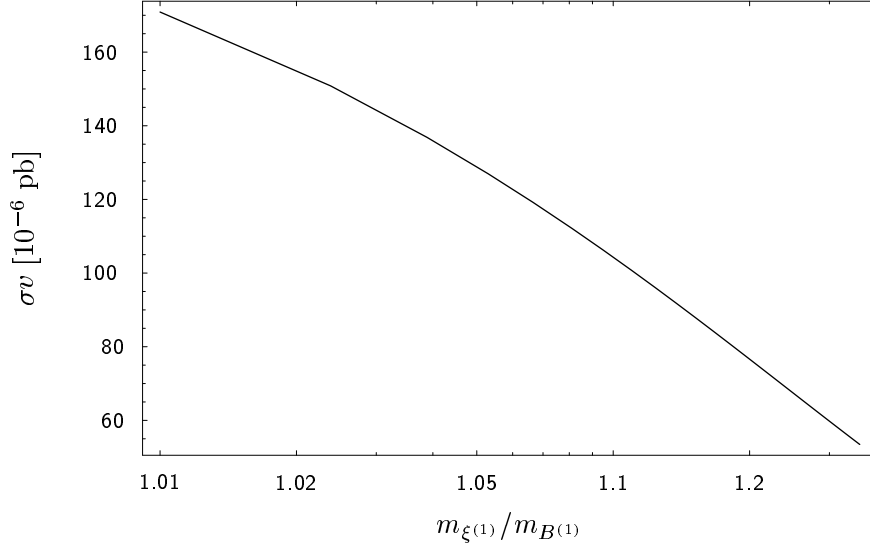


FIG. 2: The annihilation rate for $m_{B^{(1)}} = 0.8$ TeV as a function of the mass shift between the $B^{(1)}$ and KK fermions. The dependence on the $B^{(1)}$ mass is simply given by $\sigma v \propto m_{B^{(1)}}^{-2}$.

IV. CROSS SECTION

For low relative velocities v between the incoming $B^{(1)}$ particles the annihilation cross section σ diverges, but the annihilation rate is proportional to σv and finite. Assuming the same mass shift for all KK fermions, we find after summing over final and averaging over initial states:

$$\sigma v = \frac{\alpha_Y^2 \alpha_{em}^2 g_{eff}^4}{144\pi m_{B^{(1)}}^2} \left\{ 3 |B_1|^2 + 12 |B_2|^2 + 4 |B_6|^2 - 4 \text{Re} [B_1 (B_2^* + B_6^*)] \right\}, \quad (16)$$

where

$$g_{eff}^2 \equiv \sum Q^2 (Y_s^2 + Y_d^2) = \frac{52}{9}. \quad (17)$$

The sum in (17) is over all standard model charged fermions. From ordinary running of couplings, one expects $1/\alpha_{em}(1 \text{ TeV}) \sim 123$ and $1/\alpha_Y(1 \text{ TeV}) \sim 95$. In models with extra dimensions one generically expects power-law rather than logarithmic running [31], which would further enhance the cross-section. However, the deviation from the standard case only becomes significant at energy scales considerably higher than the first KK level, so we neglect this effect here. Fig. 2 shows the annihilation rate as a function of the mass difference between the $B^{(1)}$ and the KK fermions.

Until now, we have only considered diagrams containing fermion loops. There are considerably more diagrams if one also takes into account the scalar sector of the theory; neglecting

those that are related to each other by obvious symmetries, there are actually a total number of 22 different *types* of diagrams with first KK level modes. Using the FormCalc package [32], we implemented all these contributions numerically and found that they merely make up a few percent of the total cross section. Comparing this with the direct annihilation of neutralinos $\chi\chi \rightarrow \gamma\gamma$ [21], this is actually the order of magnitude one would naively expect for the total cross section when taking into account that $m_\chi/m_{B^{(1)}} \sim 10^{-2}$. The large contribution from the fermion loops thus seems to be a special feature of the KK model we have considered here. However, it is well known that neutralino annihilation into charged leptons is helicity suppressed and the process $\chi\chi \rightarrow \gamma\gamma$ is not dominated by fermions, either. This indicates that the small fermion loop contribution is a peculiarity for supersymmetry rather than its absence a special feature of the KK model.

Higher KK levels contribute with additional diagrams, but these are suppressed by the larger KK masses in the propagators. Numerically, we have checked that adding second KK level fermions only changes our previous results by a few percent. Another possibly important contribution comes from diagrams with second KK level Higgs bosons $H^{(2)}$ in the s -channel. We found, however, that for realistic mass shifts one is too far away from the $H^{(2)}$ resonance for these processes to be important. In conclusion, the analytical expression (16) for the fermion box diagrams shown in Fig. 1 is a good approximation for the whole annihilation process $B^{(1)}B^{(1)} \rightarrow \gamma\gamma$ and we expect the effect of other diagrams to be negligible compared to the astrophysical uncertainties described in the next section.

One should also note that there are two other final states of $B^{(1)}B^{(1)}$ annihilation, $Z\gamma$ and $H\gamma$, which serve as sources of monochromatic photons. Due to the high mass of the $B^{(1)}$, these can most likely not be discriminated from those from two-photon annihilation. The fermionic contribution to the $B^{(1)}B^{(1)} \rightarrow Z\gamma$ cross section is easy to compute for a given diagram. The only difference compared to the two photon case is that the Z coupling to fermions contains both a vector *and* an axial vector. From the values of these couplings we have estimated, and checked numerically, that this gives a 10% enhancement of the gamma-ray signal coming from $\gamma\gamma$ annihilation alone. The $H\gamma$ line is left for future studies.

V. OBSERVATIONAL PROSPECTS

The detection rate of $B^{(1)}$ annihilations in the GC depends strongly on the details of the galactic halo profile which, unfortunately, is to a large extent unknown. High resolution N-body simulations favor cuspy halos, with radial density distributions ranging from r^{-1} [33] to $r^{-1.5}$ [34] in the inner regions. It has further been suggested that adiabatic accretion of dark matter onto the massive black hole in the center of the Milky Way may produce a dense spike of $r^{-2.4}$ [35]. This has, however, been contested [36, 37]. On the other hand, adiabatic contraction from the dense stellar cluster, which is measured to exist near the GC, is likely to compress the halo dark matter substantially [38, 39]. This means that there is support for a rather dense halo profile very near the center - something that may be tested with the new 30m-class telescopes [40]. Bearing these uncertainties in mind, we will use the moderately cuspy (r^{-1}) profile by Navarro, Frenk and White (NFW) [33].

The gamma-ray flux from WIMP annihilation in the GC is given by [17]

$$\Phi_\gamma(\Delta\Omega) \simeq 2.92 \cdot 10^{-11} \left(\frac{\sigma v}{10^{-29} \text{ cm}^3 \text{ s}^{-1}} \right) \times \left(\frac{0.8 \text{ TeV}}{m_{B^{(1)}}} \right)^2 \langle J_{GC} \rangle_{\Delta\Omega} \Delta\Omega \text{ m}^{-2} \text{ s}^{-1}, \quad (18)$$

where σv is the annihilation rate, and $\langle J_{GC} \rangle_{\Delta\Omega}$ is a dimensionless line-of-sight integral averaged over $\Delta\Omega$, the angular acceptance of the detector. This way of writing the flux is convenient because it separates the particle physics of the particular WIMP candidate from the details of the galactic halo profile. For a NFW profile, one expects $\langle J_{GC} \rangle_{\Delta\Omega} \Delta\Omega = 0.13 b$ for $\Delta\Omega = 10^{-5}$ [41], which is appropriate for example for the H.E.S.S. telescope [7]. Here, we follow [24] and allow for an explicit boost factor b that parametrizes deviations from a pure NFW profile ($b = 1$) and may be as high as 1000 when taking into account the expected effects of adiabatic compression [39].

The direct annihilation $B^{(1)}B^{(1)} \rightarrow \gamma\gamma$ produces mono-energetic photons with an energy that is to a very good approximation given by $E_\gamma = E_{B^{(1)}} \approx m_{B^{(1)}}$. Due to the velocities of the $B^{(1)}$ particles, however, the emitted photons become Doppler-shifted and the observed signal acquires a natural linewidth of $v \sim 10^{-3}$. Current ACTs have energy resolutions of about 10 to 20 percent [6, 7]. Satellite-borne telescopes have better spectral resolution but are limited in energy range; neither Integral ($E_\gamma \lesssim 10 \text{ MeV}$) [8] nor GLAST ($E_\gamma \lesssim 300 \text{ GeV}$) [9] can reach the energies of some hundred GeV to a few TeV that are required in order to study the expected signatures of KK dark matter. The next generation of high energy

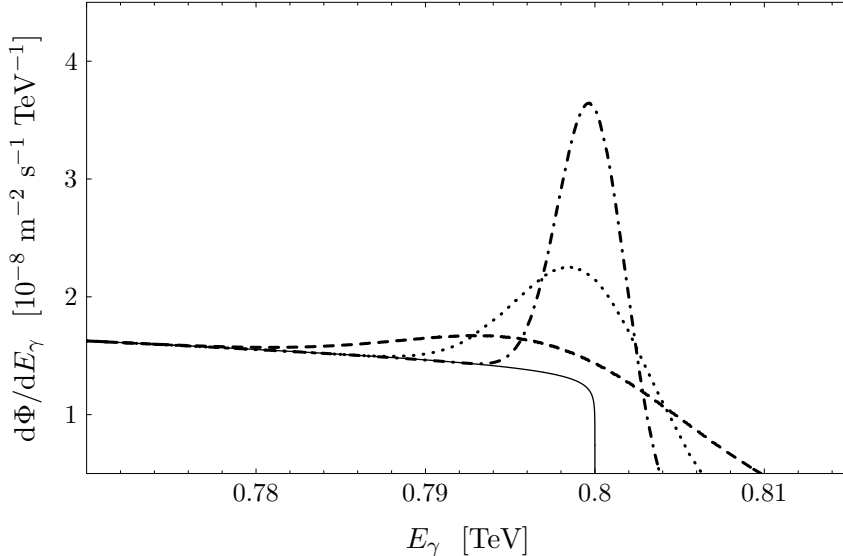


FIG. 3: The continuous gamma-ray flux that is expected from KK dark matter [24] is plotted as a solid line. To this, we have added the flux from direct annihilation as seen by a detector with an energy resolution of $2\sigma = 2\%$ (dashed), 1% (dotted) and 0.5% (dash-dotted), respectively. The actual linewidth of the signal is about 10^{-3} , with a peak value of $1.5 \cdot 10^{-7} \text{ m}^{-2} \text{ s}^{-1} \text{ TeV}^{-1}$. For all cases, we have assumed $m_{B^{(1)}} = 800 \text{ GeV}$, a mass shift $m_{\xi^{(1)}}/m_{B^{(1)}} = 1.05$, and a moderate boost factor of $b = 100$.

gamma-ray telescopes can be expected to reach even better energy resolutions, also in the TeV range, something which opens up exciting possibilities for the study of line signals from dark matter annihilations as the one described here [21, 22].

Recently, the continuous gamma-ray spectrum from KK dark matter annihilation was found to have a very promising signature [24], an almost flat energy distribution that abruptly falls off at $m_{B^{(1)}}$. Including the line signal that we have studied here, one finds a total spectrum that has an even more distinctive signature. This is shown in Fig. 3. As one can see, the next generation of experiments may well be able to see it – or falsify the KK dark matter hypothesis. Note that the *relative* strength of the line signal as compared to the continuous signal does not depend on the astrophysical uncertainties encoded in b .

In the particular model we are looking at, a dark matter particle mass as low as 300 GeV is disfavored by the WMAP relic density bound. However, it could be that the $B^{(1)}$ does not make up *all* of the dark matter; one could also imagine a different model, with equally non-suppressed couplings to fermions, that predicts a somewhat higher relic density. In both

cases one might be able to push the dark matter particle mass down to a value such that an annihilation signal like in Fig. 3 could be seen already with the GLAST satellite, taking into account its projected spectral resolution at the highest energies.

VI. CONCLUSIONS

We have studied the possible distinct signature of annihilation into mono-energetic gamma-rays of KK dark matter, one of the most interesting dark matter candidates that has appeared in recent years. We have found that with a detector of percent level energy resolution, something that is difficult but not impossible to achieve, such a “smoking gun” signal could indeed be detectable. The mass range of the KK models that derive from UED, around 0.5 - 1 TeV, places the new generation of ACTs at the center of attention. If the halo density profile has a slope of $1/r$ or more and is furthermore processed by interaction with the baryonic matter near the center of the galaxy, then this region is the obvious place to search for the gamma-ray line. On the other hand, it may be that the galaxy halo is clumpy [42] and then the best choice may be to aim at the nearest dark matter clump. The upcoming satellite experiment GLAST will have difficulties detecting energies above 300 GeV, but may do an all-sky search for the continuum signal expected in these models. The corresponding point sources without optical counterpart would be obvious targets for the observing programs of the different ACTs then in operation. An observation of the photon line would then unambiguously identify the dark matter origin, as well as give the mass of the lightest KK particle.

Much of the phenomenology would be the same for other models which do not involve Majorana fermions as dark matter. That exception happens on the other hand for neutralinos in supersymmetric models. As the Majorana nature means that the annihilation into fermions is helicity suppressed, one has to rely on a strong coupling to W^\pm in the loop to obtain large rates for the gamma line. Although there are examples in supersymmetric models of such a coupling, for example in the pure higgsino limit [17] or in split supersymmetry [43], it is not a generic feature.

In models with non-suppressed couplings to fermions, on the other hand, the calculation of the continuous gamma-ray spectrum as given in [24] would be essentially unchanged, as would the present loop calculation of the gamma line rate. In particular, the relative weight

of the two processes should be rather universal, meaning that whenever a continuous signal is claimed to have been detected, there has to be a bump at the dark matter particle mass which should stand out if the energy resolution is a few percent, or better.

Finally, one should note that the annihilation channels $B^{(1)}B^{(1)} \rightarrow Z\gamma$ and $B^{(1)}B^{(1)} \rightarrow H\gamma$ has a similar structure to the one we have studied here and is another source of monochromatic photons. We have estimated the $Z\gamma$ process to give at least a 10% enhancement of the signal that we have discussed in this article. We leave the interesting issue of the $H\gamma$ line open for later studies.

Acknowledgments

We are grateful to Thomas Hahn and Sabine Hossenfelder for helpful discussions.

Appendix

In the calculation of the loop diagrams, the following types of four-point functions appear:

$$D_0; D_\mu; D_{\mu\nu}; D_{\mu\nu\rho}; D_{\mu\nu\rho\sigma}(k_1, k_2, k_3; m_1, m_2, m_3, m_4) \\ = \int \frac{d^n q}{i\pi^2} \frac{1; q_\mu; q_\mu q_\nu; q_\mu q_\nu q_\rho; q_\mu q_\nu q_\rho q_\sigma}{[q^2 - m_1^2][(q + k_1)^2 - m_2^2][(q + k_1 + k_2)^2 - m_3^2][(q + k_1 + k_2 + k_3)^2 - m_4^2]}. \quad (19)$$

As is well-known, all these tensor integrals D_{ij} can be reduced to scalar loop integrals [44], for which closed expressions exist [45]. In certain kinematical regimes, however, the original reduction scheme [44] of Passarino and Veltman breaks down. This is for example the case for the process that we are interested in, where the two incoming $B^{(1)}$ particles have essentially identical momenta. We use the algebraic reduction scheme implemented in the LERG program [46] that adopts an extended Passarino-Veltman scheme which can cope with special situations like this.

We find that all the integrals one has to calculate for the first KK level fermion loops can be reduced to only six basic scalar integrals. Using the conventions from [45, 46] (note, however, that our signature is different from theirs), the form factors defined in section III

become

$$B_1 = \frac{8\eta^2}{\eta-1}C_0(4,0,0;\eta,\eta,\eta) - \frac{8}{\eta-1}C_0(1,0,-1;0,\eta,\eta) - \frac{16}{3(\eta+1)}B_0(4;0,0) - \frac{4(\eta-4)}{3(\eta-1)}B_0(4;\eta,\eta) + \frac{2(5\eta^2+2\eta-19)}{3(\eta^2-1)}B_0(1;0,\eta) - 2B_0(-1;0,\eta) + \frac{8}{3}, \quad (20)$$

$$B_2 = \frac{4\eta(\eta+2)}{\eta-1}C_0(4,0,0;\eta,\eta,\eta) - \frac{4\eta(2\eta+1)}{\eta-1}C_0(1,0,-1;0,\eta,\eta) - \frac{8}{3(\eta+1)}B_0(4;0,0) + \frac{2(5\eta+4)}{3(\eta-1)}B_0(4;\eta,\eta) - \frac{13\eta^2+10\eta+13}{3(\eta^2-1)}B_0(1;0,\eta) + B_0(-1;0,\eta) - \frac{8}{3}, \quad (21)$$

$$B_6 = -\frac{4\eta(\eta+2)}{\eta-1}C_0(4,0,0;\eta,\eta,\eta) + \frac{4(3\eta^2+\eta-1)}{\eta-1}C_0(1,0,-1;0,\eta,\eta) - \frac{8}{3(\eta+1)}B_0(4;0,0) - \frac{2(13\eta-4)}{3(\eta-1)}B_0(4;\eta,\eta) + \frac{41\eta^2+26\eta-31}{3(\eta^2-1)}B_0(1;0,\eta) - 5B_0(-1;0,\eta) + \frac{4}{3}, \quad (22)$$

where $\eta \equiv \left(\frac{m_f^{(1)}}{m_B^{(1)}}\right)^2$. We calculated the scalar loop integrals appearing in the expressions above as follows:

$$C_0(4,0,0;\eta,\eta,\eta) = -\frac{1}{2} \arctan^2\left(\frac{1}{\sqrt{\eta-1}}\right), \quad (23)$$

$$C_0(1,0,-1;0,\eta,\eta) = \frac{1}{2} \left\{ \text{Li}_2\left(-\frac{1}{\eta}\right) - \text{Li}_2\left(\frac{1}{\eta}\right) \right\}, \quad (24)$$

$$B_0(4;0,0) = 2 - 2 \log 2 + i\pi, \quad (25)$$

$$B_0(4;\eta,\eta) = 2 - \log \eta - 2\sqrt{\eta-1} \arctan\left(\frac{1}{\sqrt{\eta-1}}\right), \quad (26)$$

$$B_0(1;0,\eta) = 2 - \eta \log \eta + (\eta-1) \log(\eta-1), \quad (27)$$

$$B_0(-1;0,\eta) = 2 + \eta \log \eta - (\eta+1) \log(\eta+1), \quad (28)$$

where the Spence function or dilogarithm is defined by

$$\text{Li}_2(z) \equiv -\int_0^1 dt \frac{\log(1-zt)}{t} = \sum_{k=1}^{\infty} \frac{z^k}{k^2}. \quad (29)$$

[1] F. Zwicky, *Helv. Phys. Acta* **6** (1933) 110.

[2] D. N. Spergel *et al.* [WMAP Collaboration], *Astrophys. J. Suppl.* **148** (2003) 175, astro-ph/0302209.

[3] R. A. Knop *et al.*, *Astrophys. J.* **598** (2003) 102, astro-ph/0309368; A. G. Riess *et al.* [Supernova Search Team Collaboration], *Astrophys. J.* **607** (2004) 665, astro-ph/0402512 .

- [4] W. J. Percival *et al.* [The 2dFGRS Team Collaboration], *Mon. Not. Roy. Astron. Soc.* **337** (2002) 1068, astro-ph/0206256; M. Tegmark *et al.* [SDSS Collaboration], *Phys. Rev. D* **69** (2004) 103501, astro-ph/0310723.
- [5] G. Jungman, M. Kamionkowski and K. Griest, *Phys. Rept.* **267** (1996) 195, hep-ph/9506380; L. Bergström, *Rept. Prog. Phys.* **63** (2000) 793; G. Bertone, D. Hooper and J. Silk, *Phys. Rept.* **405** (2005) 279, hep-ph/0404175.
- [6] The VERITAS Collaboration, <http://veritas.sao.arizona.edu/>
The CANGAROO Collaboration, <http://icrhp9.icrr.u-tokyo.ac.jp/>
The MAGIC Collaboration, <http://wwwmagic.mppmu.mpg.de/>
- [7] The HESS Collaboration, <http://www.mpi-hd.mpg.de/hfm/HESS/>
- [8] The Integral Collaboration, <http://www.rssd.esa.int/Integral/>
- [9] The GLAST Collaboration, <http://www-glast.sonoma.edu/>
- [10] D. P. Finkbeiner, astro-ph/0409027.
- [11] S. W. Barwick *et al.*, *Astrophys. J.* **482** (1997) L191, astro-ph/9703192; S. Coutu *et al.*, *Astropart. Phys.* **11** (1999) 429, astro-ph/9902162.
- [12] A. J. Tylka, *Phys. Rev. Lett.*, **63** (1989) 840; M. S. Turner and F. Wilczek, *Phys. Rev. D*, **42** (1990) 1001; M. Kamionkowski and M. S. Turner, *Phys. Rev. D* **43** (1991) 1774; E. A. Baltz and J. Edsjö, *Phys. Rev. D* **59** (1999) 023511, astro-ph/9808243; J. L. Feng, K. T. Matchev and F. Wilczek, *Phys. Rev. D* **63** (2001) 045024, astro-ph/0008115; E. A. Baltz, J. Edsjö, K. Freese and P. Gondolo, *Phys. Rev. D* **65** (2002) 063511, astro-ph/0109318; G. L. Kane, L. T. Wang and T. T. Wang, *Phys. Lett. B* **536** (2002) 263; G. L. Kane, L. T. Wang and J. D. Wells, *Phys. Rev. D* **65** (2002) 057701, hep-ph/0108138; H. C. Cheng, J. L. Feng and K. T. Matchev, *Phys. Rev. Lett.* **89** (2002) 211301, hep-ph/0207125; D. Hooper and G. D. Kribs, *Phys. Rev. D* **70** (2004) 115004, hep-ph/0406026; D. Hooper and J. Silk, *Phys. Rev. D* **71** (2005) 083503, hep-ph/0409104.
- [13] J. Knodlseder *et al.*, *Astron. Astrophys.* **411** (2003) L457, astro-ph/0309442.
- [14] C. Boehm, D. Hooper, J. Silk, M. Casse and J. Paul, *Phys. Rev. Lett.* **92** (2004) 101301, astro-ph/0309686; C. Boehm, P. Fayet and J. Silk, *Phys. Rev. D* **69** (2004) 101302, hep-ph/0311143; D. H. Oaknin and A. R. Zhitnitsky, *Phys. Rev. Lett.* **94** (2005) 101301, hep-ph/0406146.
- [15] S. D. Hunter *et al.*, *Astrophys. J.* **481** (1997) 205; H. Mayer-Hasselwander *et al.*, *Astron. Astrophys.* **335** (1998) 161.

- [16] G. Bertone, G. Servant and G. Sigl, Phys. Rev. D **68** (2003) 044008, hep-ph/0211342. A. Cesarini, F. Fucito, A. Lionetto, A. Morselli and P. Ullio, Astropart. Phys. **21** (2004) 267, astro-ph/0305075; W. de Boer, M. Herold, C. Sander, V. Zhukov, A. V. Gladyshev and D. I. Kazakov, astro-ph/0408272; E. A. Baltz and D. Hooper, hep-ph/0411053.
- [17] L. Bergström, P. Ullio and J. H. Buckley, Astropart. Phys. **9** (1998) 137, astro-ph/9712318.
- [18] K. Tsuchiya *et al.* [The CANGAROO Collaboration], Astrophys. J. **606** (2004) L115, astro-ph/0403592; K. Kosack *et al.* [The VERITAS Collaboration], Astrophys. J. **608** (2004) L97, astro-ph/0403422; F. Aharonian *et al.* [The H.E.S.S. Collaboration], Astron. Astrophys. **425** (2004) L13, astro-ph/0408145.
- [19] D. Hooper, I. de la Calle Perez, J. Silk, F. Ferrer and S. Sarkar, JCAP **0409** (2004) 002, astro-ph/0404205; D. Horns, Phys. Lett. B **607** (2005) 225 [Erratum-ibid. B **611** (2005) 297], astro-ph/0408192.
- [20] W. de Boer, M. Herold, C. Sander and V. Zhukov, Eur. Phys. J. C **33** (2004) S981, hep-ph/0312037.
- [21] L. Bergström and H. Snellman, Phys. Rev. D **37** (1988) 3737; S. Rudaz, Phys. Rev. D **39** (1989) 3549; G. F. Giudice and K. Griest, Phys. Rev. D **40** (1989) 2549; L. Bergström and P. Ullio, Nucl. Phys. B **504** (1997) 27, hep-ph/9706232; Z. Bern, P. Gondolo and M. Perelstein, Phys. Lett. B **411** (1997) 86, hep-ph/9706538.
- [22] M. Urban, A. Bouquet, B. Degrange, P. Fleury, J. Kaplan, A. L. Melchior and E. Pare, Phys. Lett. B **293** (1992) 149, hep-ph/9208255; P. Ullio and L. Bergström, Phys. Rev. D **57** (1998) 1962, hep-ph/9707333.
- [23] P. Gondolo, J. Edsjö, P. Ullio, L. Bergström, M. Schelke and E. A. Baltz, JCAP **0407** (2004) 008, astro-ph/0406204.
- [24] L. Bergström, T. Bringmann, M. Eriksson and M. Gustafsson, Phys. Rev. Lett. **94** (2005) 131301, astro-ph/0410359.
- [25] T. Appelquist, H. C. Cheng, and B. A. Dobrescu, Phys. Rev. D **64** (2001) 035002, hep-ph/0012100.
- [26] H. C. Cheng, K. T. Matchev and M. Schmaltz, Phys. Rev. D **66** (2002) 036005, hep-ph/0204342..
- [27] G. Servant and T. M. P. Tait, Nucl. Phys. B **650** (2003) 391, hep-ph/0206071.
- [28] I. Antoniadis, Phys. Lett. B **246** (1990) 377.

- [29] K. Agashe, N. G. Deshpande and G. H. Wu, *Phys. Lett. B* **514** (2001) 309, hep-ph/0105084; A. J. Buras, M. Spranger and A. Weiler, *Nucl. Phys. B* **660** (2003) 225, hep-ph/0212143; A. J. Buras, A. Poschenrieder, M. Spranger and A. Weiler, *Nucl. Phys. B* **678** (2004) 455, hep-ph/0306158.
- [30] H. C. Cheng, K. T. Matchev and M. Schmaltz, *Phys. Rev. D* **66** (2002) 056006, hep-ph/0205314.
- [31] K. R. Dienes, E. Dudas and T. Gherghetta, *Phys. Lett. B* **436** (1998) 55, hep-ph/9803466.
- [32] T. Hahn and M. Perez-Victoria, *Comput. Phys. Commun.* **118** (1999) 153, hep-ph/9807565. T. Hahn, *Comput. Phys. Commun.* **140** (2001) 418, hep-ph/0012260;
- [33] J. F. Navarro, C. S. Frenk and S. D. M. White, *Astrophys. J.* **462** (1996) 563, astro-ph/9508025.
- [34] B. Moore, T. Quinn, F. Governato, J. Stadel and G. Lake, *Mon. Not. Roy. Astron. Soc.* **310** (1999) 1147, astro-ph/9903164.
- [35] P. Gondolo and J. Silk, *Phys. Rev. Lett.* **83** (1999) 1719, astro-ph/9906391.
- [36] P. Ullio, H. S. Zhao and M. Kamionkowski, *Phys. Rev. D* **64** (2001) 043504, astro-ph/0101481.
- [37] M. Milosavljevic and D. Merritt, *Astrophys. J.* **563** (2001) 34, astro-ph/0103350.
- [38] O. Y. Gnedin and J. R. Primack, *Phys. Rev. Lett.* **93** (2004) 061302, astro-ph/0308385.
- [39] F. Prada, A. Klypin, J. Flix, M. Martinez and E. Simonneau, astro-ph/0401512.
- [40] N. N. Weinberg, M. Milosavljevic and A. M. Ghez, astro-ph/0404407.
- [41] A. Cesarini, F. Fucito, A. Lionetto, A. Morselli and P. Ullio, *Astropart. Phys.* **21** (2004) 267, astro-ph/0305075.
- [42] J. Silk and A. Stebbins, *Astrophys. J.* **411** (1993) 439; L. Bergström, J. Edsjö, P. Gondolo and P. Ullio, *Phys. Rev. D* **59** (1999) 043506, astro-ph/9806072; C. Calcaneo-Roldan and B. Moore, *Phys. Rev. D* **62** (2000) 123005, astro-ph/0010056; L. Bergström, J. Edsjö and C. Gunnarsson, *Phys. Rev. D* **63** (2001) 083515, astro-ph/0012346; A. M. Green, S. Hofmann and D. J. Schwarz, *Mon. Not. Roy. Astron. Soc.* **353** (2004) L23, astro-ph/0309621.
- [43] A. Arvanitaki and P. W. Graham, hep-ph/0411376.
- [44] G. Passarino and M. J. G. Veltman, *Nucl. Phys. B* **160** (1979) 151.
- [45] G. 't Hooft and M. J. G. Veltman, *Nucl. Phys. B* **153** (1979) 365.
- [46] R. G. Stuart, *Comput. Phys. Commun.* **48** (1988) 367; R. G. Stuart and A. Gongora, *Comput. Phys. Commun.* **56** (1990) 337; R. G. Stuart, *Comput. Phys. Commun.* **85** (1995) 267.